Clinical Rheumatology (2019) 38:2637–2645
https://doi.org/10.1007/s10067-019-04580-8

ORIGINAL ARTICLE

A preliminary analysis of microRNA profiles in the subchondral bone between Kashin-Beck disease and primary knee osteoarthritis

Guang-Hui Zhao[1] · Lei Yang[1,2] · Mikko J. Lammi[1,3] · Xiong Guo[1]

Received: 4 November 2018 / Revised: 7 April 2019 / Accepted: 16 April 2019 / Published online: 6 May 2019

Abstract

Introduction Kashin-Beck disease (KBD) is a chronic osteochondral disorder primarily associated with cartilage degeneration. The bone texture structure in KBD was also changed but it was not identical to primary knee osteoarthritis (OA). This study investigates the differences in microRNA (miRNA) profiles of subchondral bone collected from patients suffering from KBD in comparison with those with primary knee osteoarthritis (OA).

Methods Subchondral bone tissues were taken from four patients with KBD and four patients with primary knee OA undergoing total knee replacement. The miRNA array profiling was performed using an Affymetrix miRNA 4.0 Array, and then the target gene predictions and function annotations of the predicted targets were performed.

Results Our results showed that 124 miRNAs had lower expression levels in the subchondral bone sampled from KBD patients in comparison with OA patients. Gene ontology (GO) and KEGG pathway analyses of the predicted targets demonstrated numerous significantly enriched GO terms and signal pathways essential for bone development and integrity, such as metabolic processes, PI3K-Akt, and MAPK signaling pathways.

Conclusions Our study confirms that a large set of miRNAs are differentially expressed in the subchondral bone of patients with KBD and OA and contributes new insights into potential pathological changes in the subchondral bone of KBD patients.

Keywords Kashin-Beck disease · MicroRNAs · Osteoarthritis · Subchondral bone

Introduction

Kashin-Beck disease (KBD) is a chronic, advancing, and debilitating osteoarticular disease, which affects growth and joint cartilage [1]. The etiology of KBD is still controversial, while currently two major environmental hypotheses, selenium shortage and mycotoxin contamination of grains, and also some genetic components have been considered as risk factors for the disease [2, 3]. KBD is mostly prevalent in a finite endemic region from northeastern to southwestern China, North Korea, and some eastern parts of Russia. In China, there were approximately 0.61 million individuals suffering from KBD and a total of 37.7 million individuals at high risk of KBD from 378 counties in 13 provinces or autonomous regions (National Health and Family Planning Commission of the People's Republic of China 2015).

The basic pathological element of KBD is chondronecrosis in the epiphyseal growth plate and articular cartilage. This contributes to impaired endochondral ossification and growth retardation [4]. KBD usually occurs in children at the age of 5 years or earlier, but the symptoms and signs become more

Guang-Hui Zhao and Lei Yang contributed equally to this work and should be considered as co-first authors.

Electronic supplementary material The online version of this article (https://doi.org/10.1007/s10067-019-04580-8) contains supplementary material, which is available to authorized users.

✉ Mikko J. Lammi
mikko.lammi@umu.se

✉ Xiong Guo
guox@mail.xjtu.edu.cn

[1] Key Laboratory of Trace Elements and Endemic Diseases of National Health and Family Planning Commission, Collaborative Innovation Center of Endemic Diseases and Health Promotion in Silk Road Region, School of Public Health, Health Science Center, Xi'an Jiaotong University, Xi'an 710061, Shaanxi, People's Republic of China

[2] School of Nursing, Health Science Center, Xi'an Jiaotong University, Xi'an, Shaanxi, People's Republic of China

[3] Department of Integrative Medical Biology, University of Umeå, Umeå, Sweden

severe in adult patients due to progressive cartilage damage [2]. Osteoarthritis (OA) is the most frequent form of degenerative joint disorder and a significant cause of physical disability in the adult population [5]. OA occurs mostly in older people, and its major pathological process is articular cartilage degeneration. With the progressive loss of the articular cartilage, adult KBD patients usually show manifestations similar to those of OA, such as joint pain, morning stiffness, and limited joint motion [6, 7]. However, the diagnostic criteria for adult KBD should be distinctive from those for OA because they have different etiologies, ages of onset, and pathological features [8, 9].

The term subchondral bone means the bony components, which are located distal to calcified cartilage, and which are composed of the subchondral plate and subchondral trabecular bone [10]. In OA, the subchondral bone changes mainly include sclerosis and structural changes, and they are present at the onset and advancement of OA [11]. A previous study showed that there is necrosis of trabecula bones in patients with KBD [12]; our recent study also showed the bone texture structure in patients with KBD had clearly changed in subchondral and trabecular bone, but these micro-structural changes are not identical to OA [13]. MicroRNAs (miRNAs) are small, non-coding RNAs that are important regulators of gene expression and can modulate gene transcription rates, inhibit translation, and promote decay of target mRNAs [14]. A previous study screened the miRNA profiles of the OA subchondral bone identified several previously nonrecognized miRNAs that are involved in the subchondral bone sclerosis in OA [15].

Our previous study compared the mRNA expression in adult KBD cartilage and OA cartilage and demonstrated a number of differentially expressed mRNAs in the cartilage between the two diseases [16]. However, analysis and comparison of the miRNAs involved in the subchondral bone pathogenesis have never been performed. This study compares the miRNA profiles between the KBD and the OA subchondral bones using an Affymetrix miRNA Chip and explores the potential molecular functions of the altered miRNAs and their target genes by enrichment analysis. This is the first study to explore the potential molecular changes in the subchondral bone of KBD, and the findings will contribute to greater knowledge of the different pathological features present in the subchondral bone of KBD and OA patients.

Materials and methods

Sample collection

The ethics committee of Xi'an Jiaotong University has approved this study, and all participants of the study have given informed consent. Tibial plateaus were collected from four patients with KBD and four patients undergoing total knee replacement at Honghui Hospital of Xi'an Jiaotong University due to primary knee OA. The severity of KBD was evaluated as either second or third degree, according to the clinical diagnostic criteria of KBD (WS/T 207-2010) (National Health and Family Planning Commission of the People's Republic of China 2010, http://www.nhfpc.gov.cn/zhuz/s9500/201006/47920.shtml). An example of the clinical manifestations of a KBD patient is shown in Fig. 1. The criteria of the American College of Rheumatology were used to clinically diagnose OA patients [17]. In addition, the knee joints of all participants both from the OA and the KBD groups were classified as grade 4 based on the Kellgren-Lawrence radiographic grading criteria [18]. The patients with KBD and OA were matched for age, and Table 1 compiles the basic information of all participants.

To ensure consistency of sampling regions between the KBD and the OA groups, all the specimens for miRNA array analysis were prepared from the medial plateaus. Following the surgical collection of the tibial plateaus, a scalpel was used to carefully eliminate the trabecular bone and the articular cartilage under a microscope. Then, the harvested subchondral bone fragments were immediately flash-frozen in liquid nitrogen to prevent RNA degradation.

Total RNA extraction

Total RNA from the subchondral bone was extracted by an RNeasy Mini Kit (QIAGEN, Germany) according to the manufacturer's instructions. Briefly, the frozen subchondral bones tissues were disrupted using a mortar and pestle in liquid nitrogen followed by homogenization using a QIAshredder homogenizer. Then the samples were centrifuged at full speed for 3 min, and the supernatant was transferred to a new microcentrifuge tube. One volume of 70% ethanol was added and mixed by pipetting. Up to 700 μl of samples were transferred to an RNeasy spin column placed in a 2-ml collection tube, and then centrifuged at 10,000 rpm for 15 s. To wash the spin column membrane, 700 μl Buffer RW1 was added to the RNeasy spin column and centrifuged at 10,000 rpm for 15 s and 500 μl Buffer RPE was added to the RNeasy spin column and centrifuged at 10,000 rpm for 15 s and 2 min respectively. Then, the RNeasy spin column was placed in a new 1.5-ml collection tube; 30 μl RNase-free water was directly added to the spin column membrane and then centrifuged at 10,000 rpm for 1 min to elute the RNA. Immediately following the extraction, the quantity and purity of the total RNA were measured using a NanoDrop™ One device (Thermo Scientific, USA). Furthermore, the integrity of the total RNA was assessed by visualization of the rRNA ratio (28S/18S) using agarose gel electrophoresis.

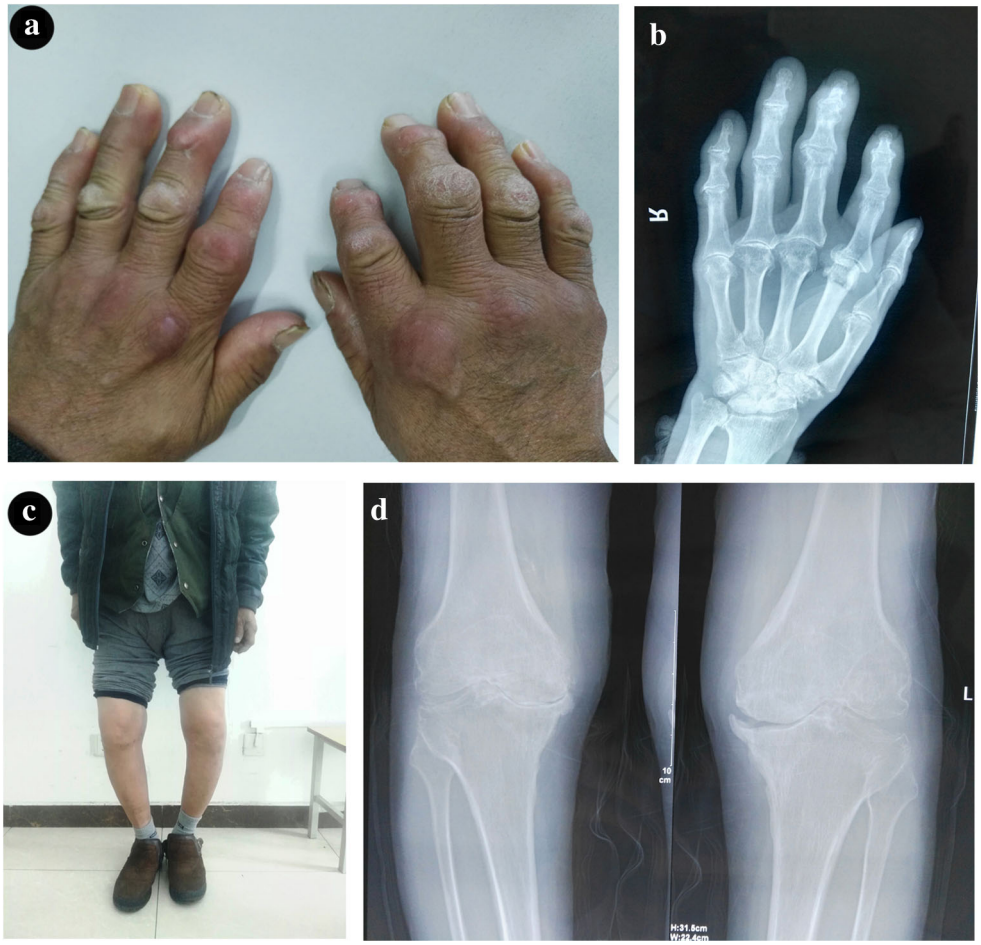

Fig. 1 The clinical and radiographic characteristics of a KBD patient (male, 59 years old). Photographic images of bilateral hands (**a**) and knees (**c**). Radiographic images of the right hand (**b**) and bilateral knees (**d**)

miRNA array profiling

The miRNA array profiling was performed using Affymetrix miRNA 4.0 Array as recommended by the manufacturer (Capitalbio, Beijing, China). Briefly, the total RNA was first labeled with biotin using a Genisphere FlashTag Labeling Kit. Then, the labeled samples were hybridized with the miRNA arrays, and the arrays were later scanned and analyzed according to the standard protocols.

Table 1 The basic characteristics of the included patients with KBD and OA

Patient No.	KBD			OA		
	Gender	Age (years)	K-L grade	Gender	Age (years)	K-L grade
1	Female	58	4	Female	56	4
2	Male	59	4	Female	58	4
3	Male	60	4	Male	62	4
4	Female	54	4	Male	60	4

K-L, Kellgren-Lawrence

miRNA array data analysis

The miRNA array profiling data analysis was carried out using the Affymetrix® GeneChip® Command Console® (AGCC) software. The quantified signals were background-corrected and normalized using a robust multiarray average algorithm [19]. The significance analysis of microarray (SAM) method was used to determine the differentially expressed miRNAs with the recruiting criteria of q-value < 0.05 and fold change ≥ 2 or ≤ 0.5. Then, the target gene predictions of the screened miRNAs were performed using 12 different prediction programs including miRWalk, Microt4, miRanda, mirbridge, miRDB, miRMap, miRNAMap, Pictar2, PITA, RNA22, RNAhybrid, and Targetscan. The predicted targets were only selected when they could be simultaneously predicted by at least six programs. In addition, function annotation of the predicted targets, including molecular function and biological process, was performed based on the gene ontology (GO) terms (http://www.geneongoloty.org/), and enriched pathways of these predicted targets were performed using the Kyoto Encyclopedia of Genes and Genomes database (KEGG) (http://www.genome.jp/kegg/).

GO and KEGG analyses were all carried out using the KEGG Orthology Based Annotation System (KOBAS 2.0, http://kobas.cbi.pku.edu.cn/).

Validation of the miRNA profiles by qRT-PCR

The miRNA array data were validated by quantitative real-time PCR (qRT-PCR). A total of six miRNAs, which satisfied the recruiting criteria of microarray data as mentioned above, were selected for the qRT-PCR. The miRNA primers are listed in Table S1. The total RNA was purified by using the mirVana™ miRNA Isolation Kit (AM1561), and then the purified total RNA was reverse transcribed to cDNA with the miRNA-specific stem-loop Megaplex RNA reverse transcriptional primer mixture. The RT reaction mix contained 100 ng of RNA, 1 μl of miRNA-specific stem-loop RT-primer, 4 μl of 5× first-strand buffer, 2 μl of 0.1 M DTT, 0.5 μl of dNTP Mixture, 1 μl of M-MLV Reverse Transcriptase, 0.2 μl of Recombinant RNasin® RNase Inhibitor and nuclease-free water in a final volume of 20 μl. The reactions were incubated at 16 °C for 10 min, 37 °C for 30 min, and 65 °C for 5 min. Subsequently, the qRT-PCR was performed using a QuantStudio™ 7 Flex RealTime PCR System (Applied Biosystems, USA) in a 20 μl mixture containing 10 μl of Power SYBR® Green PCR Master Mix (2x), 1 μl of miRNA cDNA sample, 0.5 μl of miRNA universal sense primer (10 μM), 0.5 μl of miRNA-specific anti-sense primer (10 μM), and 8 μl of nuclease-free water. The mixture was incubated at 95 °C for 10 min, followed by 40 cycles of 95 °C for 15 s and 60 °C for 1 min. The U6 gene was used as an endogenous normalization control. All assays were analyzed using the delta–delta–Ct method [20].

Results

Screening of differentially expressed miRNAs

Microarray analysis was used to compare the expression profiles of miRNAs in the subchondral bone between patients with KBD and OA. Principal component analysis (PCA) indicated a different and very clear pattern of expression between the KBD and OA groups (Fig. 2) and suggested that samples in this study were prepared appropriately. The differentially expressed miRNAs between the two groups were identified using volcano plot filtering (Fig. 3). Overall, 124 miRNAs were differentially expressed between the two groups. These miRNAs were down expressed in the subchondral bone in the KBD patients in comparison with the OA patients (q-value < 0.05 and fold change ≤ 0.5). In order to limit the contribution of the biological variability, eight differentially expressed

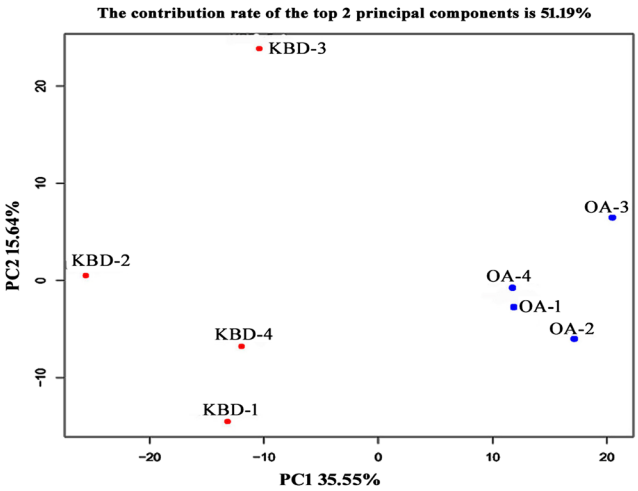

Fig. 2 Principal component analysis of the miRNA profiles in the subchondral bone from patients with KBD and OA. The red points represent samples from the KBD group, while blue points represent samples from the OA group

miRNAs were identified when a cutoff fold change of ≥ 5 or ≤ 0.2 was applied (Table 2). The full list of the differentially expressed miRNAs is provided in Table S2.

In a previous study, 30 miRNAs were differentially expressed in the subchondral bone between nonsclerotic OA vs. sclerotic OA [15]. We compared these 30 miRNAs to our microarray data. Ten miRNAs were identified, which were downregulated in the sclerotic versus nonsclerotic OA, also revealing different levels between KBD and OA, including hsa-miR-106a-5p, hsa-miR-148a-3p, hsa-miR-17-5p, hsa-miR-20b-5p, hsa-miR-30a-3p, hsa-miR-30a-5p, hsa-miR-30d-5p, hsa-miR-30e-5p, hsa-miR-708-5p, and hsa-miR-99a-3p.

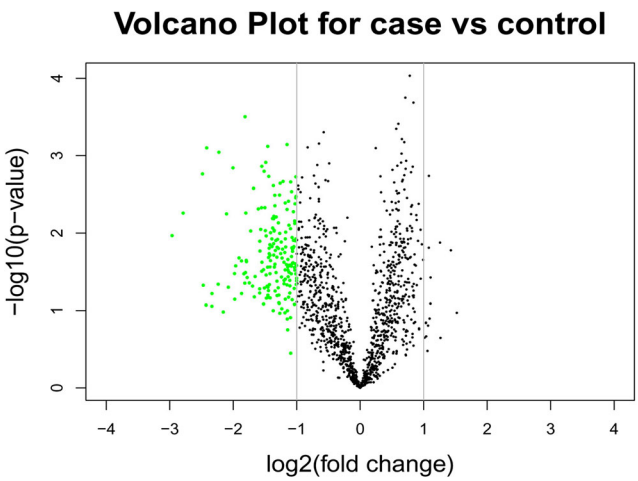

Fig. 3 Volcano plot of the differentially expressed miRNAs in the subchondral bone from patients with KBD and OA. The vertical lines correspond to –log10 (p value), and the horizontal line represents log2 (fold change). The green points in the plot represent the differentially expressed miRNAs with statistical significance

Table 2 The differentially expressed miRNAs in the subchondral bone between the patients with KBD and OA (fold change ≤ 0.2)

Gene ID	Transcript ID (array design)	*q*-value (%)	Fold change*
20502446	hsa-miR-451a	0	0.1283
20501160	hsa-miR-29c-3p	0	0.1447
20500385	hsa-miR-192-5p	0	0.1788
20501206	hsa-miR-363-3p	0	0.1803
20504379	hsa-miR-629-5p	0.50704013	0.1859
20500131	hsa-miR-17-3p	0	0.1872
20500450	hsa-miR-182-5p	0.50704013	0.1981
20503105	hsa-miR-486-5p	0.50704013	0.1983

*Fold change in the KBD patients compared with the OA patients

Target prediction and function analysis of differentially expressed miRNAs

To gather information on the general activities of the differentially expressed miRNAs, we ran analyses using the 12 different databases given above to obtain predicted target genes for all differentially expressed miRNAs. As expected, these differentially expressed miRNAs in the subchondral bone between the two groups could potentially regulate several hundred target genes. The functional analysis of the predicted target genes of the differentially expressed miRNAs was first performed using GO analysis. The top 20 GO terms of biological process and molecular function with the highest enrichment among the predicted target genes are listed in Table 3 and Table 4, respectively. The results showed that the most significant biological process was system development (GO:0048731), while the most significant molecular function was binding (GO:0005488). Several GO terms of the biological process were related to metabolism, such as regulation of metabolic process (GO:0019222), metabolic process (GO:0008152), cellular metabolic process (GO:0044237), and positive regulation of metabolic process (GO:0009893). A full list of significantly enriched GO terms of biological process and molecular function (corrected p value < 0.05) among the predicted target genesis is presented in Table S3.

A classification of the KEGG pathways of all predicted target genes involved in the differences is shown in Fig. 4. Furthermore, a total of 12 KEGG pathways were significantly enriched (corrected p value < 0.05), which included metabolic pathways, those in cancer and PI3K-Akt signaling, endocytosis, MAPK signaling cascade, Ras and Rap1 signaling routes, proteoglycans in cancer, axon guidance, cAMP signaling pathway, focal adhesion, and HTLV-I infection (Table 5).

In addition, we performed the target prediction and function analysis of the eight differentially expressed miRNAs (q-value < 0.05 and fold change ≤ 0.2), and the results of GO terms and KEGG pathways were shown in Table S4.

Table 3 Significantly enriched GO terms of biological processes of predicted target genes (Top 20 based on the corrected p value)

GO term	ID	p value	Corrected p value
System development	GO:0048731	1.40058E-51	2.75718E-48
Anatomical structure development	GO:0048856	2.04514E-50	3.43755E-47
Multicellular organismal development	GO:0007275	2.14054E-50	3.43755E-47
Regulation of metabolic process	GO:0019222	2.27005E-50	3.43755E-47
Positive regulation of cellular process	GO:0048522	3.30027E-50	4.5108E-47
Positive regulation of biological process	GO:0048518	3.43706E-50	4.5108E-47
Metabolic process	GO:0008152	1.20982E-47	1.32314E-44
Developmental process	GO:0032502	1.77906E-46	1.84329E-43
Intracellular signal transduction	GO:0035556	6.52307E-46	6.42066E-43
Regulation of signaling	GO:0023051	7.89288E-46	7.39902E-43
Regulation of cell communication	GO:0010646	1.04486E-45	9.34956E-43
Single-organism developmental process	GO:0044767	1.90478E-45	1.63032E-42
Cellular metabolic process	GO:0044237	6.2591E-44	5.13403E-41
Localization	GO:0051179	5.5913E-43	4.40281E-40
Positive regulation of metabolic process	GO:0009893	5.6377E-40	3.9637E-37
Cellular macromolecule metabolic process	GO:0044260	2.15382E-39	1.41333E-36
Regulation of cellular metabolic process	GO:0031323	2.56505E-39	1.62889E-36
Protein modification process	GO:0036211	3.43147E-39	2.04703E-36
Cellular protein modification process	GO:0006464	3.43147E-39	2.04703E-36
Nervous system development	GO:0007399	3.95421E-38	2.28949E-35

Table 4 Significantly enriched GO terms of molecular functions of predicted target genes (top 20 based on the corrected *p* value)

Term	ID	*p* value	Corrected *p* value
Binding	GO:0005488	1.47585E-90	9.68451E-87
Protein binding	GO:0005515	1.04938E-86	5.16452E-83
Ion binding	GO:0043167	6.76292E-49	8.32093E-46
Enzyme binding	GO:0019899	7.45751E-38	4.07802E-35
Anion binding	GO:0043168	2.15183E-30	7.84461E-28
Nucleoside phosphate binding	GO:1901265	9.09113E-28	2.45162E-25
Nucleotide binding	GO:0000166	1.01697E-27	2.63421E-25
Small molecule binding	GO:0036094	1.18849E-27	2.9616E-25
Purine nucleotide binding	GO:0017076	2.58763E-26	6.13737E-24
Purine ribonucleotide binding	GO:0032555	5.75438E-26	1.31722E-23
Ribonucleotide binding	GO:0032553	7.9565E-26	1.77991E-23
Purine ribonucleoside binding	GO:0032550	2.74388E-25	5.87131E-23
Purine nucleoside binding	GO:0001883	4.01755E-25	8.32521E-23
Ribonucleoside binding	GO:0032549	4.01755E-25	8.32521E-23
Carbohydrate derivative binding	GO:0097367	8.12296E-25	1.63172E-22
Purine ribonucleoside triphosphate binding	GO:0035639	8.85847E-25	1.76149E-22
Nucleoside binding	GO:0001882	1.56749E-24	3.0552E-22
Heterocyclic compound binding	GO:1901363	2.54245E-24	4.76673E-22
Metal ion binding	GO:0046872	1.55772E-23	2.71374E-21
Organic cyclic compound binding	GO:0097159	1.71415E-23	2.93432E-21

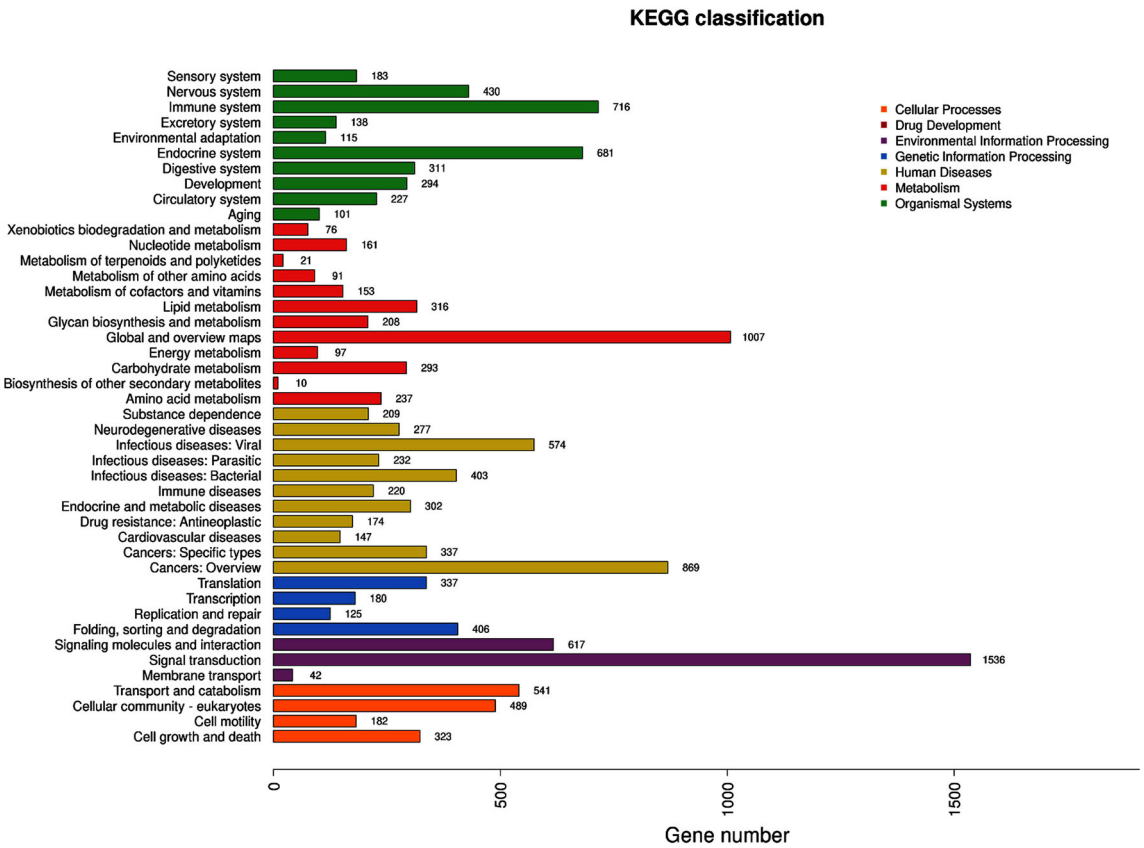

Fig. 4 Pathway assignment based on KEGG for the predicted target genes

Table 5 Significantly enriched KEGG pathways of predicted target genes

KEGG term	ID	*p* value	Corrected *p* value
Metabolic pathways	hsa01100	1.84E-08	1.64E-05
Pathways in cancer	hsa05200	6.12E-07	0.000322
PI3K-Akt signaling pathway	hsa04151	2.38E-05	0.007272
Endocytosis	hsa04144	3.21E-05	0.008773
MAPK signaling pathway	hsa04010	3.33E-05	0.008773
Ras signaling pathway	hsa04014	9.05E-05	0.017868
Proteoglycans in cancer	hsa05205	0.000116	0.019988
Rap1 signaling pathway	hsa04015	0.000133	0.019988
Axon guidance	hsa04360	0.000176	0.024901
cAMP signaling pathway	hsa04024	0.000247	0.033411
Focal adhesion	hsa04510	0.000263	0.035102
HTLV-I infection	hsa05166	0.000293	0.037523

qRT-PCR results

The microarray results were validated with the qRT-PCR for six selected miRNAs including, hsa-miR-30a-3p, hsa-miR-30a-5p, hsa-miR-99a-3p, hsa-miR-106a-5p, hsa-miR-139-5p, and hsa-miR-708-5p, which exhibited < 0.5-fold change in microarray data. The expression levels of hsa-miR-106a-5p (fold change = 0.934), hsa-miR-30a-3p (fold change = 0.896), hsa-miR-30a-5p (fold change = 0.716), hsa-miR-99a-3p (fold change = 0.884), miR-139-5p (fold change = 0.818), and hsa-miR-708-5p (fold change = 0.707) were all downregulated in the subchondral bone for KBD vs OA in PCR and showed similar expression patterns with the microarray results, confirming the validity of the microarray data.

Discussion

KBD and OA are both degenerative joint diseases, typically leading to irreversible cartilage and bone destruction. The primary clinical characteristics of KBD include pain and widening of the joints in the extremities and deformity and growth retardation at the advanced stages [6]. In adult KBD patients, pain and deformities of the joints usually occur in the larger joints, such as elbows and knees, and these features are analogous to those present in primary OA patients. However, the age of onset, symptoms, and X-ray findings are different between these two diseases [8], which suggests that they are caused by different etiologies and pathogenesis. Many studies have explored these differences pathogenesis by comparing the differences in molecules, including mRNAs [16], miRNAs [21], and DNA methylation profiles [22] between patients with KBD and OA, but all of these studies have focused on the cartilage lesions of the two diseases.

The subchondral bone alterations in parallel with the cartilage damage have been regarded as a hallmark of OA [11]. Although bone changes of KBD were observed from radiographs [13, 23], no study focused on the molecular changes of subchondral bone in KBD is available to date. Collection of joint specimens from completely normal patients is quite difficult; thus, in this study, we compared the differentially expressed miRNAs in the subchondral bone between KBD and OA. The Kellgren-Lawrence radiographic grading system was used to classify the severity of patients, unfortunately, we did not use the Range of Motion (ROM) or the WHO DAS II scale to assess the clinical backgrounds of patients. Our comprehensive microarray results clearly revealed a different miRNA expression pattern in the subchondral bone between KBD and OA and suggest that different pathological changes in the subchondral bone distinguish these two diseases.

The miRNAs have important regulatory functions in the development and integrity of both cartilage and bone. A recent study identified a total of 123 differentially expressed miRNAs (108 upregulated and 15 downregulated) in blood specimens from KBD vs. OA patients [21]. Here, we pinpointed 124 miRNAs of the subchondral bone, which were downregulated in KBD compared with OA, and ten of those were also downregulated in the sclerotic subchondral bone in comparison with the nonsclerotic subchondral bone in OA [15]. These results suggest that the subchondral bone alterations in KBD are different from OA, and many differentially expressed miRNAs in this study probably contributed to the subchondral bone lesions found in KBD. A number of these differentially expressed miRNAs have been well studied in various biological processes, for instance, miR-106a-5p, miR-148a-3p, and miR-708-5p in tumor development [24–26]. In addition, some of these miRNAs have also been studied in bone and cartilage development and homeostasis. For instance, miR-17-5p by targeting SMAD7 and miR-221 by targeting RUNX2 have been shown to be associated with the regulation of the differentiation of osteoblasts [27, 28]. miR-30a-5p promotes the apoptosis of chondrocytes in patients with OA by targeting the Akt gene [29]. Moreover, miR-335-5p appears to be a vital regulator of bone homeostasis, and there is an interrelationship between miR-335-5p expression and OA development [30]. However, the detailed actions of these miRNAs in the subchondral bone lesions of KBD warrant further study.

The enrichment analysis of the differentially expressed miRNA target genes found several vital signaling networks that are committed to the process of bone development and remodeling. These findings may help us to realize the potential mechanisms of subchondral bone alteration in KBD. In this study, GO analysis found that many terms of the biological process were related to development and metabolism, such as system and anatomical structure development, metabolic control and other cellular processes. The metabolism

processes, such as energy metabolism and lipid metabolism, have been shown to be essential mechanisms for proper bone tissue development [31]. The GO analysis also indicated that the molecular functions of these predicted genes were related to various types of molecular binding, such as protein binding, ion binding, and enzyme binding. The KEGG pathway analysis showed that the metabolic pathways were the most significantly enriched pathways. In addition, other interesting pathways, such as the PI3K-Akt, MAPK, and cAMP signaling pathways, were also recognized in this study. PI3K-Akt signaling plays an essential role both in cartilage and bone biology, and a previous study has shown induction of the PI3K/AKT route in the subchondral bone of an OA model [32]. The stimulation of the PI3K/Akt signaling cascade has also been observed in KBD patients, and it plays a role in chondrocyte apoptosis and necrosis in KBD [33]. Moreover, studies have provided evidence that MAPK signaling plays a critical role in the regulation of bone mass through the interplay of osteoblast and osteoclast differentiation [34] and that cAMP signaling is involved in osteoblast maturation and differentiation [35].

In conclusion, we compared the miRNA profiles in the subchondral bone of patients with KBD and OA. Our results demonstrated that more than a hundred miRNAs were differentially expressed in the subchondral bone of KBD and OA patients and suggest that these molecules might be possible biomarkers for discriminating between the two diseases. Along with the bioinformatics analysis, our efforts also provide insights into the regulatory alterations of miRNAs in the subchondral bone of KBD patients and the potential mechanisms that are involved. However, the main limitation is that we used a small sample size in this study which would affect the practical weight of the findings.

Acknowledgments This study was supported by the National Natural Scientific Foundation of China (NO. 81472924 and 81620108026) and the Fundamental Research Funds for the Central Universities (NO. xjj2018154).

Compliance with ethical standards

The ethics committee of Xi'an Jiaotong University has approved this study, and informed consent was obtained from all individual participants included in the study.

Conflict of interest None.

References

1. Hinsenkamp M (2001) Kashin-Beck disease. Int Orthop 25(3):133
2. Guo X, Ma WJ, Zhang F, Ren FL, Qu CJ, Lammi MJ (2014) Recent advances in the research of an endemic osteochondropathy in China: Kashin-Beck disease. Osteoarthr Cartil 22(11):1774–1783. https://doi.org/10.1016/j.joca.2014.07.023
3. Yang L, Zhao GH, Liu H, Wang X, Guo X, Lammi MJ (2016) Field synopsis and meta-analyses of genetic epidemiological evidence for Kashin-Beck disease, an endemic osteoarthropathy in China. Mol Gen Genomics 291(5):1823–1833. https://doi.org/10.1007/s00438-016-1222-z
4. Pasteels JL, Liu FD, Hinsenkamp M, Rooze M, Mathieu F, Perlmutter N (2001) Histology of Kashin-Beck lesions. Int Orthop 25(3):151–153
5. Martel-Pelletier J, Barr AJ, Cicuttini FM, Conaghan PG, Cooper C, Goldring MB, Goldring SR, Jones G, Teichtahl AJ, Pelletier JP (2016) Osteoarthritis. Nat Rev Dis Primers 2:16072. https://doi.org/10.1038/nrdp.2016.72
6. Guo X (2001) Diagnostic, clinical and radiological characteristics of Kashin-Beck disease in Shaanxi Province, PR China. Int Orthop 25(3):147–150
7. Mathieu F, Begaux F, Lan ZY, Suetens C, Hinsenkamp M (1997) Clinical manifestations of Kashin-Beck disease in Nyemo Valley, Tibet. Int Orthop 21(3):151–156
8. Li Y, Zhou Z, Shen B, Yang J, Kang P, Yang X, Liu G, Pei F (2013) Clinical features of Kashin-Beck disease in adults younger than 50 years of age during a low incidence period: severe elbow and knee lesions. Clin Rheumatol 32(3):317–324. https://doi.org/10.1007/s10067-012-2115-0
9. Schepman K, Engelbert RH, Visser MM, Yu C, de Vos R (2011) Kashin Beck disease: more than just osteoarthrosis: a cross-sectional study regarding the influence of body function-structures and activities on level of participation. Int Orthop 35(5):767–776. https://doi.org/10.1007/s00264-010-1043-3
10. Goldring MB, Goldring SR (2010) Articular cartilage and subchondral bone in the pathogenesis of osteoarthritis. Ann N Y Acad Sci 1192:230–237. https://doi.org/10.1111/j.1749-6632.2009.05240.x
11. Li G, Yin J, Gao J, Cheng TS, Pavlos NJ, Zhang C, Zheng MH (2013) Subchondral bone in osteoarthritis: insight into risk factors and microstructural changes. Arthritis Res Ther 15(6):223. https://doi.org/10.1186/ar4405
12. Bi HY (2002) Reexamination on histomorphology of necrosis of trabecula bones in Kashin-Beck disease. Endemic Dis Bull 17(1):5–7
13. Li W, Hirvasniemi J, Guo X, Saarakkala S, Lammi MJ (2018) Comparison of bone texture between normal individuals and patients with Kashin-Beck disease from plain radiographs in knee. Sci Rep 8(1):17510. https://doi.org/10.1038/s41598-018-35552-8
14. Yoon JH, Abdelmohsen K, Gorospe M (2014) Functional interactions among microRNAs and long noncoding RNAs. Semin Cell Dev Biol 34:9–14. https://doi.org/10.1016/j.semcdb.2014.05.015
15. Prasadam I, Batra J, Perry S, Gu W, Crawford R, Xiao Y (2016) Systematic identification, characterization and target gene analysis of microRNAs involved in osteoarthritis subchondral bone pathogenesis. Calcif Tissue Int 99(1):43–55. https://doi.org/10.1007/s00223-016-0125-7
16. Duan C, Guo X, Zhang XD, Yu HJ, Yan H, Gao Y, Ma WJ, Gao ZQ, Xu P, Lammi M (2010) Comparative analysis of gene expression profiles between primary knee osteoarthritis and an osteoarthritis endemic to Northwestern China, Kashin-Beck disease. Arthritis Rheum 62(3):771–780. https://doi.org/10.1002/art.27282
17. Altman R, Asch E, Bloch D, Bole G, Borenstein D, Brandt K, Christy W, Cooke TD, Greenwald R, Hochberg M et al (1986) Development of criteria for the classification and reporting of osteoarthritis. Classification of osteoarthritis of the knee. Diagno Ther Criteria Committee Am Rheum Assoc Arthritis Rheum 29(8):1039–1049
18. Kellgren JH, Lawrence JS (1957) Radiological assessment of osteo-arthrosis. Ann Rheum Dis 16(4):494–502
19. Irizarry RA, Hobbs B, Collin F, Beazer-Barclay YD, Antonellis KJ, Scherf U, Speed TP (2003) Exploration, normalization, and

summaries of high density oligonucleotide array probe level data. Biostatistics 4(2):249–264. https://doi.org/10.1093/biostatistics/4.2.249

20. Livak KJ, Schmittgen TD (2001) Analysis of relative gene expression data using real-time quantitative PCR and the 2(-Delta Delta C(T)) Method. Methods 25(4):402–408. https://doi.org/10.1006/meth.2001.1262
21. Wu W, He A, Wen Y, Xiao X, Hao J, Zhang F, Guo X (2017) Comparison of microRNA expression profiles of Kashin-Beck disease, osteoarthritis and rheumatoid arthritis. Sci Rep 7(1):540. https://doi.org/10.1038/s41598-017-00522-z
22. Wang W, Yu Y, Hao J, Wen Y, Han J, Hou W, Liu R, Zhao B, He A, Li P, Fan Q, Wu C, Wang S, Wang X, Ning Y, Guo X, Zhang F (2017) Genome-wide DNA methylation profiling of articular cartilage reveals significant epigenetic alterations in Kashin-Beck disease and osteoarthritis. Osteoarthr Cartil 25(12):2127–2133. https://doi.org/10.1016/j.joca.2017.08.002
23. Fu Q, Cao J, Renner JB, Jordan JM, Caterson B, Duance V, Luo M, Kraus VB (2015) Radiographic features of hand osteoarthritis in adult Kashin-Beck disease (KBD): the Yongshou KBD study. Osteoarthr Cartil 23(6):868–873. https://doi.org/10.1016/j.joca.2015.01.009
24. Wu J, Huang J, Wang W, Xu J, Yin M, Cheng N, Yin J (2017) Long non-coding RNA Fer-1-like protein 4 acts as a tumor suppressor via miR-106a-5p and predicts good prognosis in hepatocellular carcinoma. Cancer Biomark 20(1):55–65. https://doi.org/10.3233/cbm-170090
25. Jili S, Eryong L, Lijuan L, Chao Z (2016) RUNX3 inhibits laryngeal squamous cell carcinoma malignancy under the regulation of miR-148a-3p/DNMT1 axis. Cell Biochem Funct 34(8):597–605. https://doi.org/10.1002/cbf.3233
26. Monteleone NJ, Lutz CS (2017) miR-708-5p: a microRNA with emerging roles in cancer. Oncotarget 8(41):71292–71316. https://doi.org/10.18632/oncotarget.19772
27. Jia J, Feng X, Xu W, Yang S, Zhang Q, Liu X, Feng Y, Dai Z (2014) MiR-17-5p modulates osteoblastic differentiation and cell proliferation by targeting SMAD7 in non-traumatic osteonecrosis. Exp Mol Med 46:e107. https://doi.org/10.1038/emm.2014.43
28. Zhang Y, Gao Y, Cai L, Li F, Lou Y, Xu N, Kang Y, Yang H (2017) MicroRNA-221 is involved in the regulation of osteoporosis through regulates RUNX2 protein expression and osteoblast differentiation. Am J Transl Res 9(1):126–135
29. Shen PF, Qu YX, Wang B, Xu JD, Wei K, Xie ZK, Ma Y (2017) miR-30a-5p promotes the apoptosis of chondrocytes in patients with osteoarthritis by targeting protein kinase B. Zhonghua Yi Xue Za Zhi 97(39):3079–3084. https://doi.org/10.3760/cma.j.issn.0376-2491.2017.39.008
30. Tornero-Esteban P, Rodriguez-Rodriguez L, Abasolo L, Tome M, Lopez-Romero P, Herranz E, Gonzalez MA, Marco F, Moro E, Fernandez-Gutierrez B, Lamas JR (2015) Signature of microRNA expression during osteogenic differentiation of bone marrow MSCs reveals a putative role of miR-335-5p in osteoarthritis. BMC Musculoskelet Disord 16:182. https://doi.org/10.1186/s12891-015-0652-9
31. Desjardin C, Vaiman A, Mata X, Legendre R, Laubier J, Kennedy SP, Laloe D, Barrey E, Jacques C, Cribiu EP, Schibler L (2014) Next-generation sequencing identifies equine cartilage and subchondral bone miRNAs and suggests their involvement in osteochondrosis physiopathology. BMC Genomics 15:798. https://doi.org/10.1186/1471-2164-15-798
32. Lin C, Shao Y, Zeng C, Zhao C, Fang H, Wang L (2018) Blocking PI3K/AKT signaling inhibits bone sclerosis in subchondral bone and attenuates post-traumatic osteoarthritis. J Cell Physiol 233(8):6135–6147. https://doi.org/10.1002/jcp.26460
33. Du XA, Wang HM, Dai XX, Kou Y, Wu RP, Chen Q, Cao JL, Mo XY, Xiong YM (2015) Role of selenoprotein S (SEPS1) -105G>A polymorphisms and PI3K/Akt signaling pathway in Kashin-Beck disease. Osteoarthr Cartil 23(2):210–216. https://doi.org/10.1016/j.joca.2014.11.017
34. Sharma AR, Jagga S, Lee SS, Nam JS (2013) Interplay between cartilage and subchondral bone contributing to pathogenesis of osteoarthritis. Int J Mol Sci 14(10):19805–19830. https://doi.org/10.3390/ijms141019805
35. Liou SF, Hsu JH, Chu HC, Lin HH, Chen IJ, Yeh JL (2015) KMUP-1 promotes osteoblast differentiation through cAMP and cGMP pathways and signaling of BMP-2/Smad1/5/8 and Wnt/beta-catenin. J Cell Physiol 230(9):2038–2048. https://doi.org/10.1002/jcp.24904